Biomed. Technik
45 (2000), 20-25

O. Wendt[1]
J. Oellinger[2]
T. C. Lüth[3]
R. Felix[2]
U. Boenick[1]

The Effects of the Use of Piezoelectric Motors in a 1.5-Tesla High-Field Magnetic Resonance Imaging System (MRI)

Effekte von piezoelektrischen Motoren in einem 1,5-Tesla-Hochfeld-Magnetresonanztomographen (MRT)

[1]Technische Universitat Berlin, Institut fur Mikrotechnik und Medizintechnik
[2]Universitatsklinikum Charité Berlin, Campus Virchow-Klinikum, Strahlen- und Poliklinik
[3]Universitatsklinikum Charité Berlin, Campus Virchow-Klinikum, Klinik für Mund-, Kiefer- und Gesichtschirurgie

Key words: MRI – artefacts – piezomotor – ultrasonic motor – MR sequences

Purpose: This paper presents the results of an experimental investigation with two different rotatory piezomotors in a closed 1.5 Tesla high-field MRI. The focus of the investigation was on testing the functionality of these motors within the MRI and to determining the image interference they caused.
Materials and Methods: To obtain a differentiated estimate of the interference the motors were tested in both the passive (turned off, i.e. without current flow) and active (turned on, i.e. with current flow) state during MRI scanning. Three different types of sequences were used for the test: Spin-Echo (SE), Gradient-Echo (GE) and Echo-Planar Imaging (EPI). A plastic container filled with a gadolinium-manganese solution was used for representation of the artefacts. The motors investigated were placed parallel to the container at predetermined distances during the experiment.
Results and Conclusions: The results show that the motors investigated suffered no functional limitations in the magnetic field of the MRI but, depending on the type of motor, the measurement distance and the state of the motor, the motors had different effects on the sequence images. A motor in the off-state placed immediately next to the object to be measured mainly causes artefacts because of its material properties. If, on the other hand, the piezomotor is in the on-state images with strong noise result when the motor is immediately next to the object being measured. The images regain their normal quality when the motor is approximately. at a distance of 1 m from the object being investigated. Driving the motor inside the MRI, therefore, is only to be recommended during the pauses in scanning: this delivers artefact-free images if minimal, motor-specific distances are kept to. With regard to the three different types of sequences it was determined that the SE sequence was the least sensitive and the EPI sequence the most sensitive to disturbance. The GE sequence showed only minimal differences to the SE sequence with regard to signal-to-noise ratios. Since it requires considerably shorter scan-times it can be considered to be the most effective type of sequence under these conditions.

Schlusselworter: MRT, Artefakte, Piezomotor, MR-Sequenzen

Dieser Beitrag zeigt die Ergebnisse einer experimentellen Untersuchung mit zwei unterschiedlich aufgebauten Piezomotoren in einem geschlossenen 1,5-Tesla-Hochfeld-Magnetresonanztomographen. Im Vordergrund standen die funktionelle Überprüfung dieser Motoren innerhalb des MRT und die Ermittlung des Störeinflusses auf die Bildgebung. Zur differenzierten Abschätzung der Störeinwirkungen wurden die Motoren im passiven (stromlos) und im aktiven (stromführend) Zustand während des Scanbetriebes eingesetzt. Gescannt wurde mit drei unterschiedlichen Sequenztypen (Spin-Echo (SE), Gradienten-Echo (GE), Echo-Planar-Imaging (EPI)). Zur Darstellung der Artefakte wurde ein mit Gd-Mn-Lösung gefüllter Kunststoffbehälter verwendet, zu dem die zu untersuchenden Motoren während der Versuchsdurchführung in definierten Abstanden parallel verschoben wurden.
Die Ergebnisse sind, daß die untersuchten Motoren keine funktionellen Einschränkungen im Magnetfeld des MRT zeigten, jedoch in Abhängigkeit vom Motortyp, Meßabstand und Motorzustand unterschiedlich große Störungen in den Schnittbildern verursacht wurden. So zeigen die Ergebnisse, daß ein stromfreier Motor, in nächster Nähe zum Meßobjekt plaziert, hauptsächlich Artefakte aufgrund seiner Materialeigenschaften hervorruft. Ein strombetriebener Piezomotor dagegen führt in nachster Nähe zum Meßobjekt zu stark verrauschten Schnittbildern, die erst bei Entfernungen ab ca. 1 m vom Meßobjekt wieder normale Abbildungsqualitäten annehmen. Ein Motorbetrieb innerhalb des MRT ist deshalb nur während der Scanpausen zu empfehlen. Er liefert dann unter Berücksichtigung motorspezifischer Mindestabstände zum Meßobjekt auch artefaktefreie Bilder. Hinsichtlich der drei verwendeten Sequenzen konnte festgestellt werden, daß die SE-Sequenz die störunempfindlichste und die EPI-Sequenz die störanfälligste war. Eine nur geringe Differenz zur SE-Sequenz, hinsichtlich der ermittelten Signal-Rausch-Verhältnisse, zeigte die verwendete GE-Sequenz, die aufgrund ihrer wesentlich kürzeren Scanzeiten als die effektivste Sequenz angesehen werden kann.

Table 1. The sequences used for the investigation with the most important parameters: FOV Field of View, RFOV Rectangular Field of View, Slice-Nr. Number of Slices, Slice-Th Slice thickness, TE Echo-Time (ms), TR Repetition Time (ms).

Sequence	FOV	RFOV	Matrix	Flip-Angle	Scan-%.	Slice-Th.	Slice-Nr.	TE	TR	Scan Time
SE	430	100	256	90	70	3	25	15	353	4 16
GE (3D)	430	100	256	25	70	3	25	4,6	25	0 54
EPI	430	100	256	31	70	3	25	18	353	0 34

Introduction

Due to the increasing importance of magnetic resonance imaging in invasive diagnostics and therapy, new technical devices have to satisfy increasingly strict requirements in this area. Since the technical devices often have to be placed along with the patient into the magnetic field – for example, when they are used as diagnostic aids – they can cause image disturbances in the form of artefacts because of their material and functional features, which can make a precise diagnosis difficult. In further pursuit of a general subject dealt with in an earlier paper in which the effects of different design materials placed in the magnetic field of a 1.5 Tesla high-field magnetic resonance tomograph were investigated [1], the focus of interest in the present paper was the functional suitability of electric driving elements when they are placed in the magnetic field of a 1.5 Tesla high-field magnetic resonance tomograph and their effect on image quality. Since most conventional electrical motors cannot be placed in a MRI due to their ferromagnetic parts and its physical function mode, special motor designs had to be found. A search of the literature and inquiries made at firms [2–5] led to the conclusion that piezoelectric motors would be especially suitable for employment in strong magnetic fields due to their functional independence of magnetic fields and their usual lack of ferromagnetic parts. Two motors constructed essentially out of ceramic materials, plastics and non-ferromagnetic metal alloys were investigated. The motors were AC-driven over special motor drivers with frequencies in the kHz range. The particular goal of this study was to investigate the two differently designed rotator piezomotors in a 1.5 Tesla magnetic field with regard to their suitability, functionality and the possible disturbance of images resulting from material susceptibility and induced magnetic fields. As a basis for comparison of imaging stability, different MR sequences were evaluated: Spin-Echo (SE), Gradient-Echo (GE) and Echo-Planar Imaging (EPI). The motors were investigated both in the off-state and the on-state.

Materials and Methods

The investigation was carried out with a 1.5 Tesla high-field MRI of the Philips Company (Gyroscan ACS-NT). As transmitting and receiving coil the internal Q-Body coil of the MRI were used. For evaluation of the sequence-dependent image disturbances three sequences commonly used in clinical settings were chosen (Spin-Echo (SE), Gradient-Echo (GE) and Echo-Planar Imaging (EPI)). The most important sequence parameters are given in Table 1.

For representation of the artefacts a phantom made of polyethylene filled with a special gadolinium-manganese solution (0.011 mmol Gd/l; 0.157 mmol Mn^{2+}/l) was chosen. This choice was made in order to reach relaxation times comparable to those of human tissue (T_1 = 660 ms; T_2 = 60 ms). The phantom was placed on an acrylic base-plate which was fixed to the patient's table in the magnetic resonance tomograph. The basic arrangement of the experiment is shown in Figure 1.

The piezomotors investigated are shown in Figures 2 and 3; Table 2 shows their characteristic operating parameters.

Method

The positioning of the whole measuring set-up was achieved by means of a light marker in the MR tunnel such that the middle of the phantom was in agreement with the isocenter of the MRI. To avoid errors in positioning and to ensure reproducible measurements for repeated placement of the measuring set-up in the MR scanner, additional positional markings were drawn on the patient's table. At first, reference scans without placement of a motor were carried out in a transverse plane in all techniques listed in Table 1. Then each piezomotor was placed as shown in Figure 1 and first brought into direct contact with the object to be measured (measuring distance „0"). After the placement three measurements were performed in a transverse plane with the three sequences listed. Measurements were performed for each sequence three times. After a measuring interval was completed the motor was shifted 10 mm parallel to the phantom in the z-direction with the aid of a path marker or depending on the degree of formation of artefacts and the next measurement was performed. This procedure was repeated until image disturbance ceased. The measurements were performed first with the motor turned off and then with it turned on.

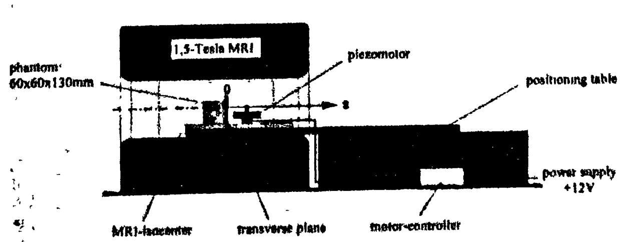

Figure 1. Experimental set-up consisting of a 1.5-Tesla magnetic resonance imaging system with a phantom and a piezomotor as object of investigation.

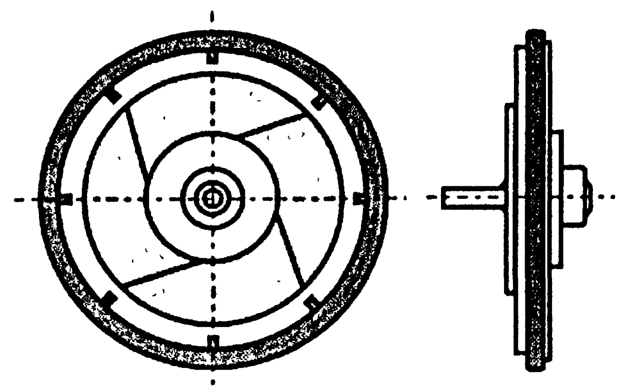

Figure 2. Piezomotor (Honda)

Table 2. Technical data of the piezomotors investigated.

Piezomotor	HSC 34 SC 02 (Honda)	USR 45 (Shinsei)
Operating voltage of the drivers, in V	DC 12	DC 12
Operating frequency in KHz	52	43
Rated number of revolutions in min^{-1}	200	130
Rated torque in Nm	0,024	0,1
Diameter in mm	46,5	50
Total height in mm	20	40,5

Results

Depending on the type of motor, the state of the motor (turned on or off) and the distance between the motor and the phantom image, disturbances of different intensity resulted. Placing a motor that was off, i.e. with no current flow, inside the MRI led basically to signal extinctions in the form of dark zones as well as contour deformations, especially when the motor was directly next to the phantom. On the other hand, a piezomotor that was on, i.e. under current, led – when the motor was directly next to the phantom – to images so deformed by noise that the test object could hardly be recognized. The image quality became normal only when the motor had been removed to a relatively large distance from the test object. The excess noise occurred both when the motor was in continual operation and when it was turned on during the scan. Below are two images showing artefacts and image disturbance for two motor states. The motor model (Shinsei), sequencing technique (GE), slice and distance from the phantom (30 mm) are the same in both images.

For determination of the maximum degree of artefact formation in each measuring sequence in the transverse plane a section close to the edge of the phantom side facing the motor was chosen. The evaluation was in general over the signal-to-noise ratio (SNR) in the section under investigation. This was by means of Equation 1 with $I_{phantom}$ being the mean signal intensity in the phantom and $R_{environment}$ being the standard deviation of the intensity of the surrounding noise field:

$$SNR = I_{phantom}/R_{environment} \quad (1)$$

In order to obtain intensity and noise values with a maximal reproducibility a constant rectangular window of measurement (ROI = Region Of Interest) was placed in the transverse section under investigation and in the surrounding noise field. The size of the ROI in the phantom and the field of noise was the same and corresponded to the liquid-filled area of the phantom in the transverse section. The SNR value of the reference measurement (phantom-measurement without motor) was defined as 100 %.

The measurement results are shown in Diagrams 1–4 below, with the SNR values of every set of measurements being given in relation to the distance of the motor from the phantom or to the first section for which the results could be evaluated. The table shows that with increasing distance of the motor from the phantom the image disturbances decreased, which is reflected in the approach of the SNR values to the reference values with increasing distance. Since there are considerable differences between the results obtained for the motor when it was on and when it was off, two characteristic curves were calculated for each motor based on the state of the motor (on or off).

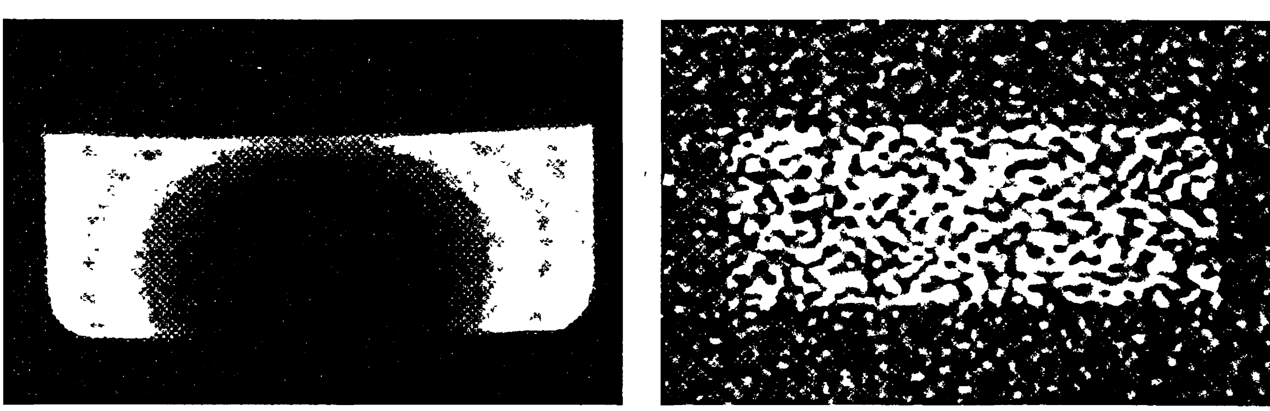

Figs. 4 a,b. Left figure: Artefacts with motor turned off, 30 mm distance to phantom, GE sequence; right figure: Image disturbances for the same motor and position, with motor on.

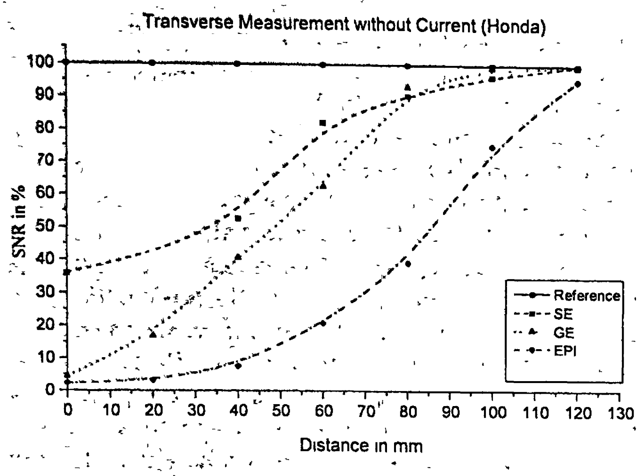

Diagram 1. Imaging disturbance caused by the Honda piezomotor in the off-state distinguished by type of imaging sequence used: SE, GE and EPI.

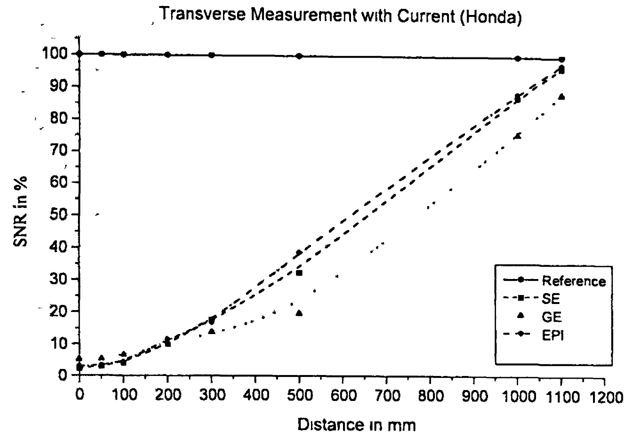

Diagram 2. Imaging disturbance caused by the Honda piezomotor in the on-state distinguished by type of imaging sequence used: SE, GE and EPI.

Since the evaluation of the section images had minor deviations ($\Delta_{SNR} = 2.5$ %), the diagrams are based on mean values.

Diagram 1 shows the characteristic curves for the Honda piezomotor in the off-state. Due to the fact that no current is flowing through the motor, it is the various motor materials which have an influence on the imaging. The axis values are defined as SNR value (y-axis of diagram) in its dependence upon the measurement distance between the motor and the phantom (x-axis of diagram), with the sequence techniques as characteristic curve parameter.

The next diagramm shows the MRI-characteristic of the Honda piezomotor when it is in the on-state. Because of the significantly greater influence on the image (by appr. a factor of 10) – as the characteristic shows – the measurements were performed at greater distances from the phantom (x-axis of diagram) than when the motor was in the off-state.

Diagrams 3 and 4 show the Shinsei motor in the off-state and the on-state. A comparison with the Honda motor shows that here greater image disturbances arise, so that correspondingly greater minimal distances have to be kept to in order to obtain interference-free images.

Discussion

A search of the literature with regard to the usability of electric motors in MRIs showed that piezoelectric motors (ultrasonic motors) might prove suitable. Two motors of this type (Honda, Shinsei) were tested using different imaging techniques both to determine the suitability of piezoelectric motors for use in MRI-systems and to investigate their influence on image quality.

The first result obtained was that the motors functioned without faults in the magnetic field of a 1.5 Tesla MRI, both before and during scanning. Independent of the influence the motors have on image quality, the-

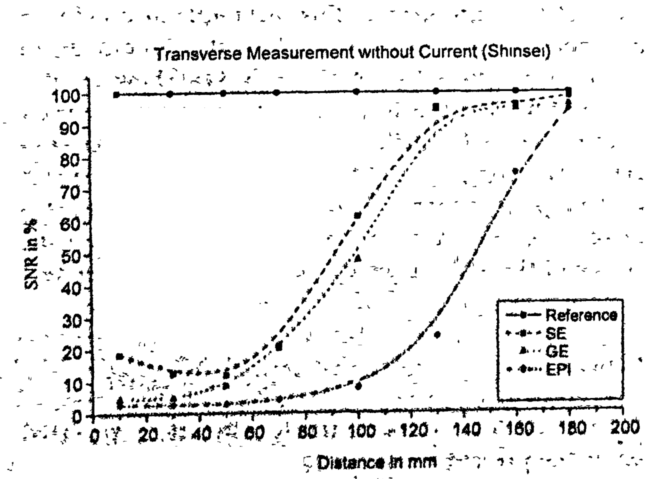

Diagram 3. Imaging disturbance caused by the Shinsei piezomotor in the of-state distinguished by type of imaging sequence used: SE, GE and EPI.

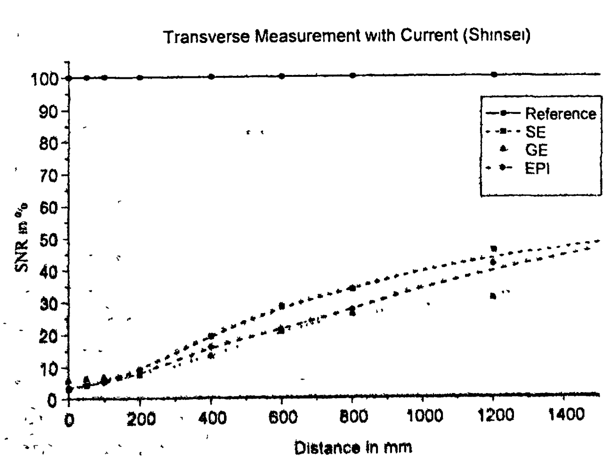

Diagram 4. Imaging disturbance caused by the Shinsei piezomotor in the on-state distinguished by type of imaging sequence used: SE, GE and EPI.

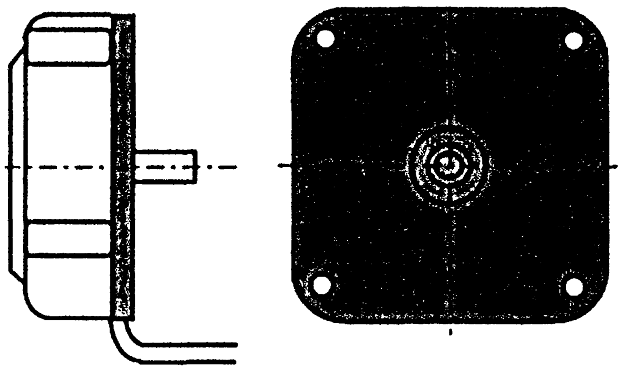

Figure 3. Piezomotor (Shinsei).

refore, they can be used, for example, for positioning within the MRI. Both motors became warmer as the operating periods increased, with the Shinsei motor becoming considerably warmer than the Honda motor due to its housing and its greater motor power. If the motor is going to be used for a longer period a check of its temperature over the housing should be made or a means of ventilation by fan provided. When the motors are manually moved in the magnetic field of the MRI minimal deflection forces can arise. These were larger with the Shinsei motor than with the Honda motor due to its greater proportion of metal. The causes of these forces are the para- and diamagnetic materials used, as well as eddy currents due to the different electric conductabilities of the materials used.

The main part of the investigation involved the determination of the artefacts or the disturbances caused by these motors with respect to the MR imaging. This was done by placing the motors at given distances from a liquid-filled phantom within the image-producing area in the MRI and performing scans of transverse sections using three different types of sequences (SE, GE, EPI). Evaluation of the transverse sectional images at a level close to the surface of the phantom showed significant differences in image disturbance depending on the state of the motor (on/off) and the motor model. In the off-state minimal image artefacts resulted, especially with the Honda motor, which were caused solely by the various material susceptibilities. In contrast, a motor in the on-state led to considerable disturbances which, when the motor was directly next to the phantom, resulted only in intense noise, so that even the contours of the phantom were unrecognizable. In addition to field disturbances due to material susceptibilities, eddy forces and conductor currents, as well the high AC current needed to drive the motor, have a significant influence on the image quality.

For applications which require placing the motor close to the object under investigation, the minimal distances at which the motors caused no image disturbance were determined. In the case of a motor in the off-state the minimal distances in order to produce artefact free images were about 120 mm for the Honda motor and 180 mm for the Shinsei motor. There is no significant difference between a horizontal and a vertical motor axle position. In the on-state the minimal distance for the Honda motor was approximately 1.2 m. The considerably more powerful Shinsei motor caused stronger disturbances than the Honda motor, with only 60 % of the SNR reference value (100%) being achieved at 1.4 m. To obtain completely disturbance-free images, therefore, motors in the on-state have to be placed at a sufficient distance from the measuring area. If, however, for motors in the off-state, corresponding minimal necessary distance are kept to, artefacts caused by the motor materials can be avoided; if it necessary to activate the motor where it is directly next to the object under investigation, or when it is within the MRI these can be carried out between the pauses within the different sequences. To avoid disturbances during the scanning procedure all electric power lines leading into the motor should be deactivated.

The MR sequences used showed different sensitivities in the characteristic curves (SNR/distance) obtained. In the course of the material investigation (motors in the off-state) the results for sequence sensitivity were to those obtained in [1]. As can be seen in Diagrams 1 and 3 the sequence sensitivity for the same distance of the motor to the phantom increases from SE to GE to EPI. The course of the characteristic curve for the SE sequence in Diagram 3 cannot be explained physically, since it shows a minimum SNR value at a distance of about 50 mm (x-value of diagram) and an increase in sensitivity as the motor was moved further away from the phantom. The measurements were carried out several times and on different days, with results that were well-reproducible. The GE characteristic curve is only minimally worse than the SE characteristic curve. However, this slight difference in quality is more than made up for by the higher time resolution so that the GE sequence can be considered as the most efficient technique. The most sensitive technique proved to be EPI but if minimal distances (appr. 180–200 mm) are kept to this technique also delivers artefact-free section images. When the motors are in the on-state the characteristic curves show similar sensitivities for the test sequence types, in contrast with motors in the off-state. This suggests that the excessively strong noise obtained is largely independent of the type of sequence used, depending only on the type of motor, the state of the motor (on/off) and the distance of the motor from the object being investigated.

Conclusion

Within the framework of the investigations reported on in the present work the following conclusions can be drawn:

1. Use of either of the piezoelectric motors investigated in a 1.5 Tesla magnetic resonance tomograph as

a driving apparatus or for positioning would seem to be acceptable.

2. If placement of the motor directly next to the object being examined is necessary use of it in the on-state during scanning leads to images that are unusable for diagnostic purposes due to the resulting intense noise.
3. A scanning operation should only be carried out with the electric system of the motor deactivated or with the motor turned off to avoid images with intense noise.
4. If the placement of a motor in the off-state close to the object under investigation is necessary the minimal distances for artefact-free images have to be kept to.
5. Of the sequence types investigated the SE sequence yields the most precise section images. However, since the quality of the GE sequences is only slightly inferior to that of the SE sequences but the time resolution of the GE sequence is significantly greater than that of the SE sequence, the GE sequence can be considered as the more efficient technique.

References:

[1] Oellinger, J.; O. Wendt, C. Siewert, T. C. Lüth, R. Felix, U. Boenick: Effekte von paramagnetischen und diamagnetischen Materialien in einem 1,5-Tesla-Hochfeld-Magnetresonanztomographen (MRI). Biomedizinische Technik 43 (1998) 10.

[2] McCarly, H.: Piezoelectric Drive Functions in Strong Magnetic Field. Design News, Okt.91.

[3] Schaaf, U.; G. Diefenbach, R. Colson: Piezoelectric motors for automotive applications. Philips Symposium Automotive Systems, 1995.

[4] Catalogue: Shinsei-Ultrasonic Motor, 1998.

[5] Catalogue: Honda Electronics, 1998.

932

Address of correspondence.
Dipl.-Ing. O. Wendt
Institut für Mikrotechnik und Medizintechnik
Technische Universität Berlin
Dovestr. 6, D-10587 Berlin
Telefon +49 30 3 14-2 16 08
Telefax +49 30 3 14-2 10 98
E-Mail: owendt@bmt1.kf.tu-berlin de